Multiple optical traps with a single laser beam using a simple and inexpensive mechanical element

J. A. Dharmadhikari, A. K. Dharmadhikari, V. S. Makhija and D. Mathur*

Tata Institute of Fundamental Research, 1, Homi Bhabha Road, Mumbai 400 005, India

An ordinary wire mesh is utilized to facilitate the creation of multiple optical traps (tweezers) for manipulation of small micron or sub-micron particles. Each of the traps formed in this manner is continuous and the entire array is amenable to easy control. Our method is simple to implement, inexpensive, and obviates the need to timeshare a laser beam among a set of positions, as is required in conventional multiple traps. We quantify the utility of our method by demonstrating that our continuous multiple traps are of essentially uniform strength. By way of illustrating the utility of our multiple traps, a single live red blood cell (RBC) of diameter ~8 μm was held at two locations on its surface; upon varying the inter-trap spacing, distortion in cell shape provides a ready means of studying the elastic properties of the RBC membrane under physiological conditions.

Keywords: Lasers, multiple traps, optical trap, optical tweezers.

OPTICAL traps (tweezers) work on the principle of creating an intensity gradient by strongly focusing a laser beam. The resulting intensity gradient produces a field gradient that helps trap a dielectric particle. Upon moving the physical focus point, the trapped particle also moves. The key feature of optical tweezers is that the steep intensity gradient induces a force whose magnitude is made to be stronger than the forces that are imparted by the scattering of the laser beam from the microscopic particles. The magnitude of such gradient forces and thereby the strength of the trap, can be readily and precisely controlled by varying the laser intensity. Particle sizes ranging from tens of nanometres to a few micrometres can be trapped and manipulated using single optical tweezers[1,2]. Although optical tweezers have found numerous and diverse applications, the fact that only a single particle can be trapped with one laser beam is a constraint that is faced in many potential applications in the field of electronics, photonics and biology, where simultaneous spatial manipulation of a number of microscopic particles would be of considerable utility[3].

Multiple optical traps have potential utility in diverse applications, many of which remain to be discovered as the technique becomes more user-friendly than it is at present. Amongst applications that are already under implementation are the organization of planar assemblies of colloidal particles[4], experimental verification of new ideas in statistical mechanics[5] and quantitative determination of macromolecular interactions[6]. Dynamic holographic tweezers can transfer particles along arbitrary three-dimensional trajectories[7]. Static array of traps can continuously sort fluid-borne particles, analogous to a sieve but in non-contact fashion. This kind of sorting is extremely sensitive to particle size. A brief review on various applications of multiple traps has been recently published[8].

Hitherto-existing multiple optical traps[4–9] rely on one of the following strategies:

(i) the use of multiple laser beams;
(ii) splitting a single laser beam into two parts by means of a polarizing beam splitter and then combining the two beams at the aperture of the objective;
(iii) steering a single beam at different locations using either rotating mirrors[10] or acousto-optic modulator[11]; or
(iv) making use of diffractive optical elements such as computer-generated holograms that split the input beam into a pre-selected desired pattern[12–16].

Though the use of multiple laser beams appears to be the obvious choice to create multiple traps, the cost factor and the associated difficulty of aligning more than a single beam through a 100X microscope objective have proved to be serious experimental impediments. Furthermore, it is known that diffractive optical devices synthesize multiple optical traps with arbitrary intensity profiles[12]. Recourse has to be taken to computational methods that have been developed to derive the holographic pattern required for any given intensity distribution in the specimen plane[13]. Moreover, traps using diffractive optical elements have a fixed configuration, for a static hologram. In order to alter the trap configuration one has to physically change the diffractive optical element. Only in the case of a dynamic hologram can the configuration be easily altered; such traps are fully automated[14,15]. The use-

fulness of holography-based optical trapping has been extended to generate three independent, movable, doughnut-mode trapping beams with an addressable liquid crystal spatial light modulator (SLM) by Reicherter et al.[16]. Improvement in SLM technology and real-time hologram calculations has made it possible to create an array of as many as 400 optical traps and has facilitated three-dimensional manipulation of higher-order beams in multiple traps[17].

We note that in the case of the acousto-optic deflector (AOD), even though one can control two traps independently, the traps are not continuous, their intermittency depending on the frequency of the AOD. Moreover, the considerable technical difficulties that are encountered in working with AODs have precluded widespread availability of multiple trap technology. Dynamic holographic traps are capable of producing various patterns[18] that offer nanometre resolution in real time[19]; however the computation time that is required for generating the appropriate hologram remains a practical limitation in many cases. Fast generation rates (>30 Hz) have been reported that are based on ferroelectric materials[20], but the associated complexity (and cost) is much higher than for a simple trap that we report in the following.

Our simple method is based on the use of a metallic wire mesh to create multiple optical traps by diffracting an incident laser beam[21]. Diffraction of monochromatic light from an array of apertures is well known. The possibility of regularizing spatial modulation of a femtosecond laser pulse has been recently demonstrated using a wire mesh[22,23], in the context of studies on the propagation of intense light through condensed media. In the method that we present here, a wire mesh is used to create a diffraction pattern in two-dimensional plane that lies perpendicular to the laser propagation direction.

This pattern is reproduced at specific distances that are obtained from Fresnel's diffraction law. Such a diffraction pattern, when focused using a microscope objective, produces multiple arrays, each of which constitutes an optical trap. The multiple traps can be translated and rotated by fixing the wire mesh on a translation stage whose motion can be precisely controlled, and the inter-trap distance can be readily altered. One of many potential applications of our multiple trap technology is demonstrated with reference to a red blood cell that is trapped at two separate locations along its 8 μm diameter. Altering the distance between the two trapping spots enables membrane elasticity measurements to be made and opens the potential for providing new insights into the trapping dynamics of a live cell kept under physiological conditions.

Experimental details

Figure 1 is a schematic representation of our experimental single-beam, multiple-trap set-up. Practical details con-

cerning many of the components that we utilize have been published in the context of a single trap that we have used recently in single-cell studies[24]. In brief, an Nd–YVO$_4$ laser beam (1 mm diameter) was passed through a beam expander so as to produce a parallel beam of 10 mm diameter. This beam is then passed through two lenses (L1 and L2) that form a telescopic arrangement, and through a 45° mirror onto a large numerical aperture 100X microscope objective (NA = 1.3). A nickel wire mesh of dimension 175 μm × 175 μm, with 95 μm wire thickness and 50% transmission, was placed in the beam path near L1. The multiple beams that result from diffraction were used to trap and manipulate polystyrene beads. Altering the mesh–L1 distance changes the relative trap positions.

In order to quantify the properties of our multiple traps, a second laser (670 nm, 1 mW) was used to image the trapped beads (2 μm diameter) onto a calibrated quadrant photodiode (QPD; Figure 1). We used a 2 mm aperture to make the laser spot circular, followed by a beam expander. The 670 nm beam co-propagated with our trapping beam (1064 nm). We used a 1064 nm blocking filter and a 670 nm bandpass filter before the QPD. We placed a microscope cover slip containing material to be trapped (shown in Figure 1) on a piezo-driven translational stage that was capable of being electronically driven to a precision of 100 nm. The signal from the QPD was measured using a 100 MHz bandwidth, four-channel, digital storage oscilloscope (Tektronix TDS 2014). Data were acquired for 0.5 s.
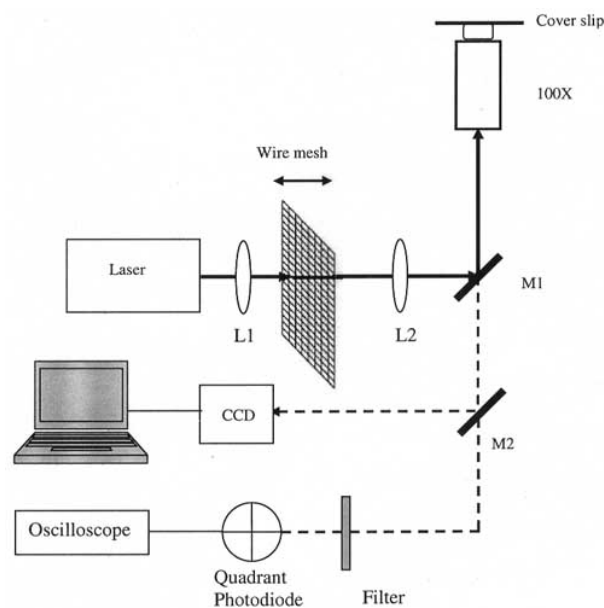
Figure 1. Single laser beam set-up to create multiple traps with a wire mesh (175 μm × 175 μm, wire thickness 95 μm). M1 and M2 are mirrors, while L1 and L2 are lenses. A second laser (670 nm) was used for calibration of stiffness of individual traps (see text).

For a bead held by the trap and subjected to a drag force proportional to its velocity, the power spectrum for the displacement of the trapped bead along the x-coordinate can be written as[25]

$$S_x(f) = \frac{k_B T}{\gamma \pi^2 (f_c^2 + f^2)}. \tag{1}$$

Equation (1) has a Lorentzian form of the type that is depicted in Figure 2, as a smooth curve in a typical power spectrum that we measured in our experiments: at low frequencies the line of slope zero meets the higher-frequency line of slope –2 at a characteristic (corner) frequency f_c, a parameter that can be readily measured.

The experimental spectrum shown in Figure 2 is the result of averaging over ten individual datasets. The trap stiffness, k_{trap} can be readily obtained once a value of f_c is deduced from the measured power spectrum:

$$k_{trap} = 2\pi\gamma f_c, \tag{2}$$

where γ for a spherical bead is simply $6\pi\eta r$, with η denoting the viscosity of the water medium containing beads of radius r. Methods of power spectrum analysis for calibration of optical traps that utilize position sensitive detectors (like a QPD) are now standardized and have been cogently summarized in the context of new developments in a series of recent reports[26–28].

Results and discussion

The diffraction pattern obtained from a mesh can be understood by considering a rectangular array of apertures with dimensions b_x and b_y that are separated by widths w_x
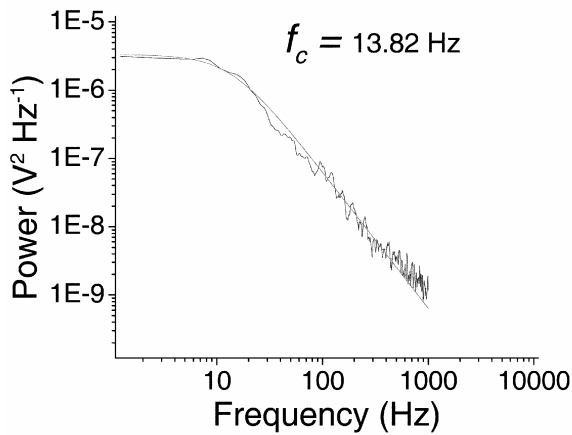
and w_y, lying in the $x - y$ plane. A plane monochromatic wave travelling along the z-direction incident normally on the above mentioned rectangular array will diffract the light. The intensity of light that is diffracted at angle α with respect to the z-axis in the $x - y$ plane is given by the Fraunhofer relation[29]:

$$I_x(\alpha) = \left(\frac{b_x \sin\beta_x}{\beta_x} \frac{\sin(N\delta_x)}{\sin\delta_x} \right)^2, \tag{3}$$

where

$$\beta_x = (b_x \pi / \lambda)\sin\alpha, \ \ \delta_x = (p_x \pi / \lambda)\sin\alpha, \tag{4}$$

and N is the number of diffracting elements contributing to the optical field, λ is the wavelength of light used, and $p_x = b_x + w_x$ is the pitch of the array. The first term in eq. (3) is the Fraunhofer diffraction pattern due to a single slit of width b_x and the second term is the intensity distribution resulting from interference between the diffraction patterns produced by the array of N such slits whose pitch is p_x. In case of a square mesh (of the type we have used), the intensity due to diffraction along the x and y directions is the same ($I_x = I_y$). The diffracted intensity in case of an array of apertures not only depends on the size of aperture b, but also on the pitch of the array p. The spacing between individual traps can be altered by varying the wire mesh size. We also carried out experiments with different sizes of the mesh placed before L1. The spacing between the two consecutive traps reduces when the mesh size is increased.

We now discuss controlling the distance between two adjacent traps for a given mesh. The spacing between two adjacent traps can be altered by placing the wire mesh between the telescopic arrangement (1 : 1). It is evident from Figure 3 a–d that as the distance between the mesh and L1 increases, the distance between adjacent traps reduces. This is because increase in the distance between L1 and the mesh reduces the size of the laser beam that is incident on the mesh. The mesh is thus subjected to a convergent beam of light rather than a parallel beam. The second lens, L2, collects the divergent light from the mesh and converts it back into a parallel beam. In Figure 3 a, when the mesh is close to L1 (~1 cm), adjacent traps are separated by 8 μm. When the mesh is 5 cm away from the lens, this distance reduces to 6 μm. For 11 cm separation, the distance between the two traps reduces to only 3.4 μm (Figure 3 d). Thus, one can exercise good control on the individual location of the multiple traps.

It should be noted that the central spot corresponds to the zeroth-order diffraction while the immediately adjacent spots correspond to first-order diffraction. If the incident laser power was further increased, second-order diffraction spots also became visible. Diffraction efficiency remained constant with distance between the mesh and

Figure 2. Typical power spectrum measured when a trapped polystyrene bead of 2 μm diameter undergoes Brownian motion. f_c = 13.82 Hz denotes the corner frequency that is used to determine trap stiffness (0.0021 pN nm^{-1}) along the x-coordinate.

the objective: as long as all of the individual traps were from the same diffraction order, there was no variation in trap efficiency. Figure 4 shows how the spacing between adjacent traps varies as a function of the distance between the mesh and the lens L1.

In order to quantify the uniformity of trap stiffness in our multiple traps, we performed experiments using 2 μm diameter polystyrene spheres suspended in distilled water. The trapping events were captured in a real-time movie. Figure 5 a–d are typical snapshots from the movie that shows beads trapped at different locations. We observed trapping at the location of both first- and sec-
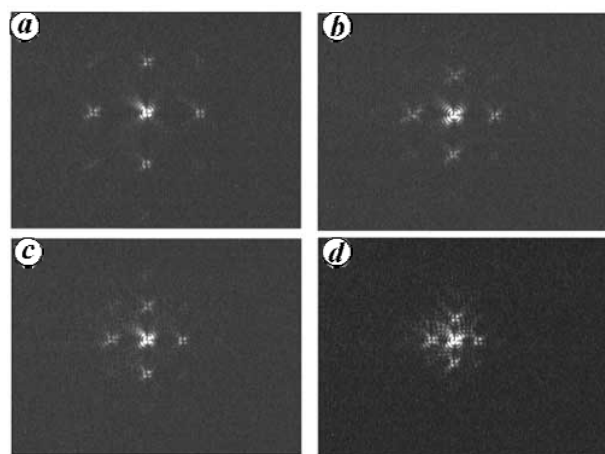

Figure 3. Photographs showing variation of distance between adjacent traps accomplished by varying the distance between the wire mesh and the lens L1: (*a*) 1 cm, (*b*) 5 cm, (*c*) 7 cm and (*d*) 11 cm. The corresponding distances between adjacent traps were (*a*) 8 μm, (*b*) 6 μm, (*c*) 5 μm, and (*d*) 3.4 μm. See the freely accessible movie clip at: http://video.yahoo.com/video/play?vid=407748.
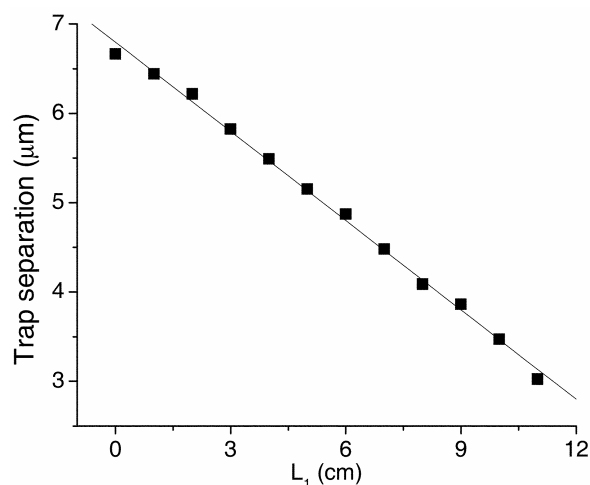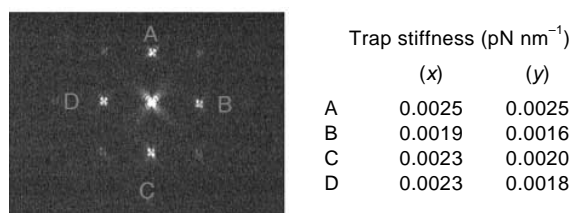

Figure 4. Variation of the spacing between two adjacent traps as a function of distance, L1, between the mesh and the lens. The slope of the straight-line fit to the data is –0.33.

ond-order diffraction. The trapped beads could be translated using a precision translation stage, as seen in the movie clip. We have quantified the trap stiffness of each of our multiple traps by making measurements of power spectra along the horizontal (x) and vertical (y) directions, and illustrative data are presented for four traps, denoted A, B, C and D in Figure 6. The trapped bead at each position (as indicated in Figure 6) was translated so as to coincide with the centre of the QPD. We note that our stiffness values pertain to incident power of 30 mW. We were, however, able to use considerably larger power levels.

Trap stiffness was essentially of the same magnitude for each of the four locations. Further, as the mesh was translated from $z = 0$ cm to $z = 11$ cm, variation in the measured laser power after the 100X objective was <5%. Thus, by translating the mesh there is negligible change in power at the trap locations shown in Figure 6 (first-order diffracted spots).
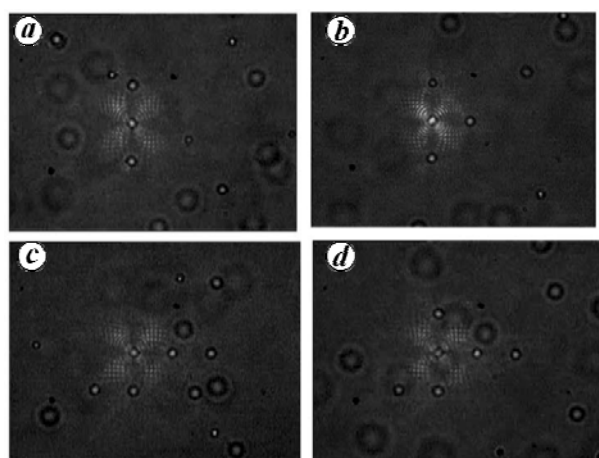
Figure 5. Snapshots from a real-time movie showing trapping of 2 μm size polystyrene beads in multiple traps. The distance between the lens and the wire mesh was kept constant (5 cm). Beads trapped at different locations are recognized as sharply focused circular images: trapping of (*a*) 3 beads, (*b*) 4 beads at zeroth- and first-order diffraction locations, (*c*) 5 beads and (*d*) 6 beads at zeroth-, first-, and second-order diffraction locations. See the freely accessible movie clip at http://video.yahoo.com/video/play?vid=407741.

	Trap stiffness (pN nm^{-1})	
	(x)	(y)
A	0.0025	0.0025
B	0.0019	0.0016
C	0.0023	0.0020
D	0.0023	0.0018

Figure 6. Stiffness (in units of pN nm^{-1}) measured for individual traps at first-order diffraction locations denoted by A, B, C, and D along mutually orthogonal directions, x and y. Stiffness for the central trap was 0.0038 pN nm^{-1} (x-direction) and 0.0036 pN nm^{-1} (y-direction).
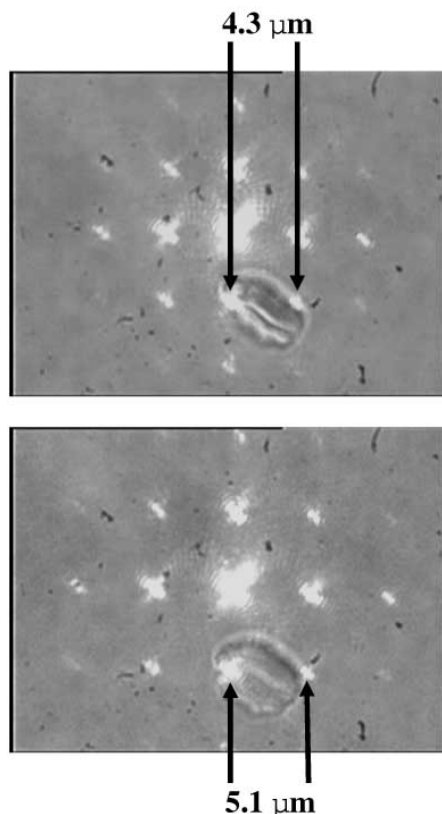
Figure 7. Trapping of a live red blood cell at two locations, indicated by vertical arrows. (Top) Distance between the two trapping locations is 4.3 μm. (Bottom) Distance increased to 5.1 μm. Note the alteration in cell shape that accompanies the stretching by 0.8 μm. See the freely accessible movie clip at http://video.yahoo.com/video/play?vid=407761.

Thus, we demonstrate the utility of a simple wire mesh in creating continuous multiple traps of essentially uniform strength. By way of illustration of just one of the many possible utilities of our simple multiple trap, we show in Figure 7 the trapping of a live red blood cell (RBC) of ~8 μm diameter, at two different locations along its surface. In the top frame the distance between the two trapping locations is 4.3 μm and in the bottom frame it is increased to 5.1 μm. As already discussed, such a change in inter-trap distance was readily accomplished in our scheme (Figure 4). Note the alteration in cell shape that accompanies the stretching by 0.8 μm. Such changes in cell shape can be used to investigate the elastic properties of the cell membrane, under physiological conditions. This is one example wherein stretching is accomplished along two trapping positions. As is clear from Figure 7, it would be a simple matter to also trap the RBC using three or more, trapping locations, so that two-dimensional stretching can be probed. Such experiments would be difficult to perform using the micropipette technique that has hitherto been considered as the main one available for such studies.

Optical trapping of RBCs has attracted much recent attention[30–32]. Euler buckling-induced folding and rotation of red blood cells in a single optical trap has been studied[30] and it has been established that upon trapping a single, live RBC, its normal biconcave disk shape folds into a rod-like shape[31]. If the trapping laser light is circularly polarized, the folded RBC rotates[32]. A model based on geometric considerations, using the concept of Euler buckling instability, has been utilized to capture the essential physics of the folding phenomenon[30]. RBC rotations in an optical trap that uses circularly polarized laser light has been rationalized in terms of a Poincaré sphere[30]. It is important and interesting to explore the role of terms beyond the harmonic one treated in the energy expressions used in the existing analysis[30]. In order to probe these effects experimentally, it becomes important to quantify in-plane and out-of-plane rotational motion of a trapped RBC; trapping of more than a single location on the cell surface becomes mandatory, and experimentally accessible using the multiple trapping scheme that we have demonstrated here.

1. Ashkin, A., Dziedzic, J. M., Bjorkholm, J. E. and Chu, S., Observation of a single-beam gradient force optical trap for dielectric particles. *Opt. Lett.*, 1986, **11**, 288–290.
2. Neuman, K. C. and Block, S. M., Optical trapping. *Rev. Sci. Instrum.*, 2004, **75**, 2787–2809.
3. Visscher, K., Gross, S. P. and Block, S., Construction of multiple-beam optical traps with nanometer-resolution position sensing. *IEEE J. Sel. Top. Quantum Electron.*, 1996, **2**, 1066–1076.
4. Gong, M. C., Terray, A. and Marr, D. W. M., Morphological control of mesoscale colloidal models. *Fluid Phase Equilibria*, 2001, **185**, 157–163.
5. Faucheux, L. P., Bourdieu, L. S., Kaplan, P. D. and Libchaber, A. J., Optical thermal ratchet. *Phys. Rev. Lett.*, 1995, **74**, 1504–1507.
6. Varma, R., Crocker, J. C., Lubensky, T. C. and Yodh, A. G., Entropic colloidal interactions in concentrated DNA solutions. *Phys. Rev. Lett.*, 1998, **81**, 4004–4007.
7. Curtis, J. E., Koss, B. A. and Grier, D. G., Dynamic holographic optical tweezers. *Opt. Commun.*, 2002, **207**, 169–175.
8. Grier, D. G., A revolution in optical manipulation. *Nature*, 2003, **424**, 810–816.
9. Visscher, K. and Block, S., Versatile optical traps with feedback control. *Methods Enzymol.*, 1998, **298**, 460–489.
10. Sasaki, K., Koshioka, M., Misawa, H., Kitamura, N. and Masuhara, H., Pattern formation and flow control of fine particles by laser-scanning micromanipulation. *Opt. Lett.*, 1991, **16**, 1463–1465.
11. Brouhard, G. J., Schek III, H. T. and Hunt, A. J., Advanced optical tweezers for the study of cellular and molecular biomechanics. *IEEE Trans. Biomed. Eng.*, 2003, **50**, 121–125.
12. Korda, P., Spalding, G. C., Dufresne, E. R. and Grier, D. G., Nanofabrication with holographic optical tweezers. *Rev. Sci. Instrum.*, 2002, **73**, 1956–1957.
13. Liesener, J., Reicherter, M., Haist, T. and Tiziani, H. J., Multifunctional optical tweezers using computer-generated holograms. *Opt. Commun.*, 2000, **185**, 77–82.
14. Dufresne, E. R. and Grier, D. G., Optical tweezer arrays and optical substrates created with diffractive optics. *Rev. Sci. Instrum.*, 1998, **69**, 1974–1977.
15. Dufresne, E. R., Spalding, G. C., Dearing, M. T., Sheets, S. A. and Grier, D. G., Computer-generated holographic optical tweezer arrays. *Rev. Sci. Instrum.*, 2001, **72**, 1810–1816.

RESEARCH ARTICLES

16. Reicherter, M., Haist, T., Wagemann, E. U. and Tiziani, H. J., Optical particle trapping with computer-generated holograms written on a liquid-crystal display. *Opt. Lett.*, 1999, **24**, 608–610.
17. Igasaki, Y. *et al.*, High efficiency electrically-addressable phase-only spatial light modulator. *Opt. Rev.*, 1999, **6**, 339–344.
18. Wang, G., Wen, C. and Ye, A., Dynamic holographic optical tweezers using a twisted-nematic liquid crystal display. *J. Opt. A: Pure Appl. Opt.*, 2006, **8**, 703–708.
19. Grier, D. G. and Roichman, Y., Holographic optical trapping. *Appl. Opt.*, 2006, **45**, 880–887.
20. Hossack, W. J., Theofanidou, E., Crain, J., Heggarty, K. and Birch, M., High-speed holographic optical tweezers using a ferro-electric liquid crystal microdisplay. *Opt. Express*, 2003, **11**, 2053–2059.
21. Dharmadhikari, J. A., Dharmadhikari, A. K. and Mathur, D., 2006, http://arxiv.org/abs/physics/060714.
22. Schroeder, H., Liu, J. and Chin, S. L., From random to controlled small-scale filamentation in water. *Opt. Express*, 2004, **12**, 4768.
23. Dharmadhikari, A. K., Rajgara, F. A., Mathur, D., Schroeder, H. and Liu, J., Efficient broadband emission from condensed media irradiated by low-intensity, unfocused, ultrashort laser light. *Opt. Express*, 2005, **13**, 8555–8564.
24. Dharmadhikari, J. A. and Mathur, D., Using an optical trap to fold and align single red blood cells. *Curr. Sci.*, 2004, **86**, 1432–1437.
25. Sheetz, M. P., Laser tweezers in cell biology. *Methods Cell Biol.*, 1998, **55**, 138.
26. Berg-Sørensen, K., Peterman, E. J. G., Weber, T., Schmidt, C. F. and Flyvbjerg, H., Power spectrum analysis for optical tweezers. II: Laser wavelength dependence of parasitic filtering, and how to achieve high bandwidth. *Rev. Sci. Instrum.*, 2006, **77**, 063106–063110.
27. Tolić-Nørrelykke, S. F., Schäffer, E., Howard, J., Pavone, F. A., Jülicher, F. and Flyvbjerg, H., Calibration of optical tweezers with positional detection in the back focal plane. *Rev. Sci. Instrum.*, 2006, **77**, 103101–103111.
28. Berg-Sørensen, K. and Flyvbjerg, H., Power spectrum analysis for optical tweezers. *Rev. Sci. Instrum.*, 2004, **75**, 594–612.
29. Jenkins, F. A. and White, H. E., In *Fundamentals of Optics*, McGraw Hill, New York, 1957, 3rd edn, p. 330.
30. Ghosh, A. *et al.*, Euler buckling-induced folding and rotation of red blood cells in an optical trap. *Phys. Biol.*, 2006, **3**, 67–70.
31. Dharmadhikari, J. A., Roy, S., Dharmadhikari, A. K., Sharma, S. and Mathur, D., Torque-generating malaria-infected red blood cells in an optical trap. *Opt. Express*, 2004, **12**, 1179–1185.
32. Dharmadhikari, J. A., Roy, S., Dharmadhikari, A. K., Sharma, S. and Mathur, D., Naturally occurring, optically driven, cellular rotor. *Appl. Phys. Lett.*, 2004, **85**, 6048–6050.